This document is the accepted version of a published work that appeared in final form in Langmuir, after technical editing by the publisher. To access the final edited and published work, see https://doi.org/10.1021/acs.langmuir.5b01442

Liposome-Templated Hydrogel Nanoparticles as Vehicles for Enzyme-Based Therapies.

*Sara Bobone,[a] Ermanno Miele,[a, §] Barbara Cerroni,[a] Daniela Roversi,[a] Alessio Bocedi,[a] Eleonora Nicolai,[b, c] Almerinda Di Venere,[b, c] Ernesto Placidi,[d, e] Giorgio Ricci,[a] Nicola Rosato[b, c] and Lorenzo Stella[a, *]*

a) Dipartimento di Scienze e Tecnologie Chimiche, b) Dipartimento di Medicina Sperimentale e Chirurgia, c) NAST center, d) Dipartimento di Fisica, Università di "Roma Tor Vergata", e) Istituto di Struttura della Materia - CNR, via fosso del Cavaliere 100, 00133, Roma, Italy.

§ Present address: Nanostructures Department, Istituto Italiano di Tecnologia (IIT), 16163 Genova, Italy.

*Corresponding author: Prof. Lorenzo Stella, Dipartimento di Scienze e Tecnologie Chimiche, Università di Roma "Tor Vergata", via della Ricerca Scientifica, 1; 00133 Roma, Italy. stella@stc.uniroma2.it

KEYWORDS: drug delivery, proteins, polyacrylamide, atomic force microscopy, dynamic light scattering, fluorescence recovery after photobleaching

ABSTRACT

Several diseases are related to the lack or to the defective activity of a particular enzyme and therefore these proteins potentially represent a very interesting class of therapeutics. However, their application is hampered by their rapid degradation and immunogenic side-effects. Most attempts to increase the bioavailability of therapeutic enzymes are based on formulations, in which the protein is entrapped within a scaffold structure but needs to be released to exert its activity. In this work, an alternative method will be described, designed to keep the enzyme in its active form inside a nanoparticle (NP) without the need to release it, thus maintaining the protective action of the nanoscaffold during the entire period of administration. In this approach, liposomes were used as nanotemplates for the synthesis of polyacrylamide hydrogel NPs under non-denaturing conditions, optimizing the polymer properties to obtain a mesh size small enough to limit the enzyme release, while allowing the free diffusion of its substrates and products. The enzyme Cu, Zn-superoxide dismutase was chosen as a test case for this study, but our results indicate that the approach is generalizable to other enzymes. Biocompatible, size-tunable nanoparticles have been obtained, with a good encapsulation efficiency (37%), in which the enzyme maintains its activity. This system represents a promising tool for enzyme-based therapy, which would protect the protein from antibodies and degradation, while allowing it to exert its catalytic activity.

INTRODUCTION

Several diseases are related to the lack or to the defective activity of a particular enzyme,[1,2] which in principle could be administered to the patients to treat such disorders. Enzymes have also several other important potential therapeutic applications as anticoagulant, anti-inflammatory, antibacterial, anticancer and amyloid-degrading drugs.[1,3,4] Although enzyme replacement therapy (ERT) has been successfully developed in some cases,[2,5] a wider application of enzymes as drugs is still hampered by the severe problems affecting this therapeutic approach, such as adverse immunologic responses,[6] short half-life of the protein-based drug in the body due to rapid elimination or to proteolytic digestion, and poor stability during the storage period.[7]

Most studies trying to enhance the bioavailability and stability of enzymes and to reduce their adverse effects are based on controlled-release formulations, where the enzyme is entrapped within a polymeric or lipid scaffold, which then is degraded and releases its therapeutic cargo inside the organism.[8] Unfortunately, the conditions required for the synthesis of some of these systems can lead to significant protein denaturation.[9] Most importantly, in these devices the enzyme must be released to exert its biological function, but in this way most of the advantages provided by the carrier are lost. An additional problem of these approaches is the release kinetics, which often involves an undesirable initial burst phase.[9]

Herein we present an alternative method that does not require enzyme release. The idea is to develop a biocompatible nanometric cage formed by a hydrophilic polymeric network with a mesh size small enough to block an enzyme, while still allowing diffusion of its substrates and products. In this way, the enzyme is entrapped in the nanoparticle (NP), protected from degradation and antibodies, and at the same time it can exert its catalytic activity. In order to synthesize the NPs in an aqueous medium to minimize protein denaturation, liposomes were exploited as nanotemplates. Phospholipid vesicles self-assemble spontaneously in water, and their dimension can be easily tuned

by extrusion through filters with pores of appropriate size. The aqueous inner volume of liposomes represents a segregated environment, in which a chemical reaction can occur separately from the bulk solution. In our case, the reaction is the gel photopolymerization and leads to the formation of hydrogel NPs inside the lipid vesicles. This approach has already been used to synthesize hydrogel NPs[10-14] and to entrap proteins in biodegradable matrices,[15] but at the best of our knowledge it has never been applied to the encapsulation of an enzyme for therapeutic purposes. The final product after the polymerization and purification processes is a device constituted by an enzyme-entrapping hydrogel core. The phospholipid bilayer, used as a template, can be removed or maintained as a possible mean to improve the intracellular delivery of the NPs.

The synthesis protocol and the gel formulation have been optimized to allow the retention of proteins inside the meshes. Acrylamide (AAm) was used as monomer and N,N'-methylene-bisacrylamide (MBA) as a crosslinker. Acrylamide-based hydrogels are widely used for drug delivery, thanks to their high biocompatibility, lack of immunogenicity, and to the possibility to finely tune the mesh size, allowing the development of different types of applications.[16,17] The use of polyacrylamide for drug preparations is allowed by the Food and Drug Administration.[18]

Although the proposed principle is rather general, the enzyme chosen as a test case for this study is Cu, Zn superoxide dismutase (SOD), both for its clinical relevance and for the small size of its substrates and products. SOD is a homodimer (molecular weight 16.3 kDa per subunit) catalyzing the dismutation of superoxide into oxygen and hydrogen peroxide, according to the following reaction:[19]

$$2\ O_2^- + 2H^+ \rightarrow O_2 + H_2O_2$$

The superoxide anion is produced in several fundamental life processes, like aerobic metabolism, oxidative phosphorylation, mitochondrial electron flux, and photosynthesis. Reactive oxygen species (ROS), such as the superoxide anion, are also generated by ionizing radiations. Unfortunately, ROS

are highly toxic for the organism: they are responsible for cell ageing and for a huge number of diseases, such as ischemia reperfusion injury, cancer, DNA damage and neurodegenerative disorders, among others.[20,21] An SOD formulation could find wide application in all these important therapeutic areas.[22] However, an SOD-based drug is still lacking:[1] human experimentation of Orgotein, *i.e.* bovine Cu, Zn SOD, has been carried out on inflammation-associated diseases, like rheumatoid arthritis and osteoarthritis.[23] However, after the clinical trials of the 1980s, the drug was retired from the market, mainly because of the immunological response against the enzyme. Although various SOD-based formulations have been proposed,[22-27] none of them has been considered for advanced clinical trials yet.[1,22]

EXPERIMENTAL

See the Supporting Information (SI).

RESULTS

Hydrogel formulation

Hydrogel composition

AAm was chosen as the building block of the polymer used in the preparation of NPs. Polyacrylamide gels have been extensively characterized, [28-30] are non-immunogenic and fully biocompatible while not biodegradable (as requested by our approach).[16,19,31] The crosslinking agent used to create the network was MBA. This monomer/crosslinker system is widely used for biomedical applications, because the mesh size of the polymeric network can be easily tuned; in

addition, the photopolymerization is a fast and easy reaction, which only needs the addition of a very small amount of photoinitiator, diethoxy acetophenone (DEAP) in our case.

The composition of polyacrylamide hydrogels can be defined by employing two parameters, T and C. T represents the total monomer+crosslinker concentration, while C is the weight fraction of crosslinker, defined according to the following equations:[32]

$$T=\frac{(monomer+crosslinker)\ weight\ (g)}{solution\ volume\ (ml)} \times 100$$

$$C=\frac{crosslinker\ weight\ (g)}{(monomer+crosslinker)\ weight\ (g)} \times 100$$

Previous studies on acrylamide-based hydrogels showed that at a fixed monomer concentration (T) the gel pore size is dependent on the amount of crosslinker (C), but also that a threshold exists, corresponding to approximately C=5%.[32-35] Above this value, bisacrylamide aggregation occurs, leading to the formation of gel inhomogeneities.[36] On the other hand, pore size is an inverse function of T,[34] but this dependence becomes weaker above T=20%, substantially reaching a plateau.[37,38]

Preliminary experiments were carried out using a T=5%, C=10% formulation, according to the protocol described by Patton and Palmer,[12] but in this case the hydrogel mesh size was too wide to efficiently entrap the SOD molecules, which diffused very rapidly out of the nanoparticles (data not shown). The same result was observed by increasing C to 30%, in agreement with the literature data showing an adverse effect of crosslinker aggregation at high C values.[32-36] To solve this problem, the hydrogel formulation was optimized using T=20% (*i.e.* a concentration of monomer + crosslinker of 0.2 mg/ml), C=5% (5 g crosslinker per 100 g monomer + crosslinker), to minimize the mesh size, according to the considerations discussed above.

Before the NPs synthesis, a bulk gel was prepared to check the effective gelation of the solution: in principle, the presence of the radical scavenger SOD could inhibit the polymerization, but this did

not occur, at least at the investigated concentration. Another control experiment, performed on an SOD solution (in the absence of any polymer precursors), showed that the UV irradiation used for polymerization during NPs synthesis did not cause any reduction in the enzymatic activity of the protein.

Fluorescence recovery after photobleaching (FRAP)

To test the efficiency of protein immobilization in the hydrogel network, FRAP experiments were carried out on a model protein, fluorescein-labeled ovalbumin: its cost is considerably lower than that of SOD, but the sizes of the two proteins are comparable (the hydrodynamic radius of ovalbumin is 31 Å,[39] as compared to 29 Å for SOD [40]).

To perform FRAP experiments, a bulk polyacrylamide gel was prepared, of the same composition used for NPs preparation (T=20%, C=5%), in which ovalbumin was entrapped, at a concentration of 30 μM. After photopolymerization, the hydrogel was left in water and extensively rinsed until the washing solution did not show any fluorescence. FRAP measurements were then performed, by cutting a thin gel slice of about 2 mm and placing it on the microscope observation glass slide. As shown in Figure 1, only a partial fluorescence recovery was observed in the time-range investigated, indicating that a large fraction of the protein was efficiently blocked within the gel network.

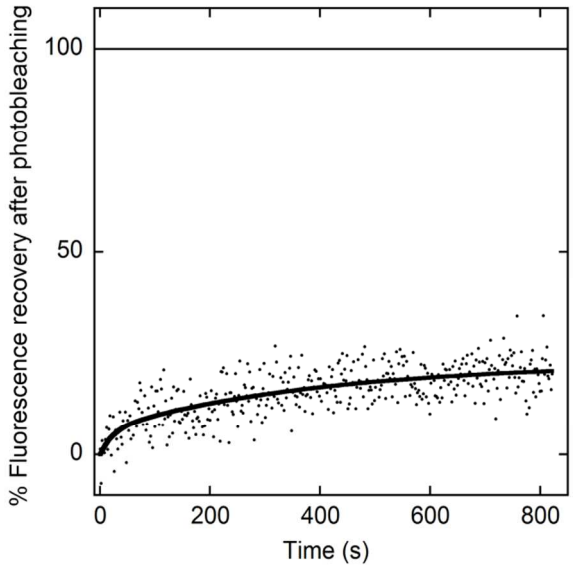

Figure 1. FRAP of protein entrapped inside the T=20%, C=5% polyacrylamide hydrogel. The continuous line represents a fit with a double exponential function (τ_1=23 s and τ_2=390 s, overall mobile fraction 23%).

SOD-membrane interaction

Several peptides and proteins exhibit a strong membrane-perturbing activity. Therefore, in principle a strong interaction between SOD and the lipid bilayer could perturb the membrane permeability, thus frustrating our approach. To rule out this hypothesis, fluorescence anisotropy measurements were performed, exploiting the intrinsic fluorescence of bovine SOD due to a Tyr residue in its sequence.[41] Free SOD in solution was titrated with phosphatidylcholine liposomes. Its fluorescence anisotropy was unaffected by the vesicle addition: the value obtained for the free enzyme (10 μM) and for the enzyme in the presence of liposomes (100 μM) were 0.10 ±0.01and 0.11 ±0.01, respectively. Based on this experiment, a significant interaction between protein and membrane can be excluded.

NPs characterization

Membrane removal by detergent addition

To obtain an effective removal of the phospholipid membrane after NPs synthesis, the detergent sodium dodecyl sulfate (SDS) was added to the particle suspension at a molar detergent to lipid ratio of 5:1 (see SI). To test the efficacy of this process, NPs were prepared including in the lipid film a small amount of phosphadityletanolamine lipids labeled with the fluorescent probe rhodamine (1% of total lipids). The fluorescence signal was recorded immediately after the preparation; the sample was then treated with SDS and submitted to an extensive dialysis cycle to remove the solubilized lipids. After the purification, a fluorescence spectrum was collected again, showing a significant signal reduction that is a clear evidence of lipid membrane removal (Figure 2).

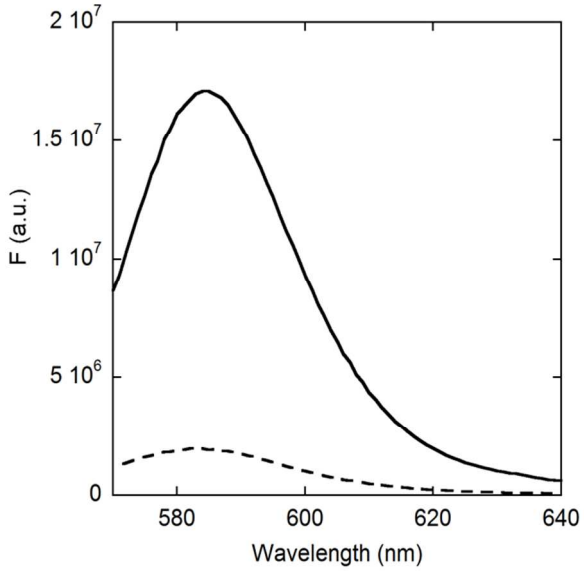

Figure 2. Fluorescence spectra of NPs with a fluorescently labeled membrane, before (continuous line) and after (dashed line) detergent addition and dialysis.

Dynamic Light Scattering Experiments

Before polymerization, the liposomes used as scaffold for NP synthesis were extruded through filters with pores of 400 nm nominal diameter, to make their dimension homogeneous. After polymerization and purification, the size of NPs was characterized by dynamic light scattering experiments before and after membrane removal. In the former case, the NPs will be called "membrane-coated", in the latter, they will be termed "naked" (Figure 3). An example of the size distribution for coated and naked NPs is reported in Figure 4. The size of samples was typically smaller than the nominal diameter of the pores used for extrusion, in agreement with previous studies,[42] with minor differences between naked and membrane-coated NPs. This measurement allows a determination of the average number of protein molecules entrapped in each NP: since no specific protein/membrane interactions are present (see above) it is reasonable to assume that during the synthesis enzyme molecules distribute uniformly in the volume outside and inside the vesicles. Therefore, from the concentration of protein in the polymerization sample (C_p) and from the typical radius of a NP (R), it can be estimated that an order of 10^2 enzyme molecules are entrapped in each particle ($N = C_p \, 4/3 \, \pi R^3 N_A$, where N_A is Avogadro's constant).

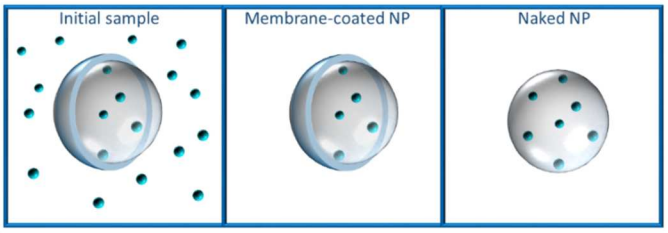

Figure 3. Schematic representation of the different configurations of the NPs sample. The whole, semitransparent sphere represents the hydrogel NP, while the smaller spheres indicate SOD molecules. The lipid bilayer is shown in section to allow the view of the liposome contents.

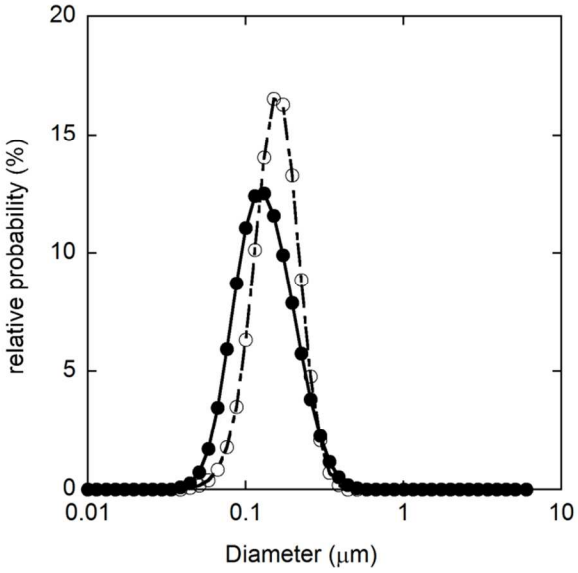

Figure 4. Size distribution of membrane-coated (empty circles, dotted line) and naked NPs (full circles, continuous line), as determined by light scattering experiments.

Atomic force microscopy (AFM) characterization

AFM experiments allowed a direct visualization of NPs. Images were collected in several regions of the mica support from different samples, obtained from NPs of diluted solutions (100 times from the stock) to avoid aggregation effects. Experiments were performed on both membrane-coated and naked NPs.

AFM images showed a large number of well-separated nanoparticles on every explored region. Two representative images are reported in Figure 5 (naked NPs) and 6 (membrane-coated NPs).

Images acquired from samples constituted of membrane-coated NPs showed that each nanoparticle is surrounded by a region with a very regular height (Figure 6) compatible with the thickness of a phospholipid bilayer (about 4 nm). This suggests that the membrane lost its integrity during the deposition and drying process and that the lipid molecules attached to the surface around the particles.

The size distribution profiles calculated from AFM images (Figure 5 B reports the results obtained for naked NPs) are representative of dried hydrogels, which lost their hydration water and became smaller with respect to the hydrated sample in solution.

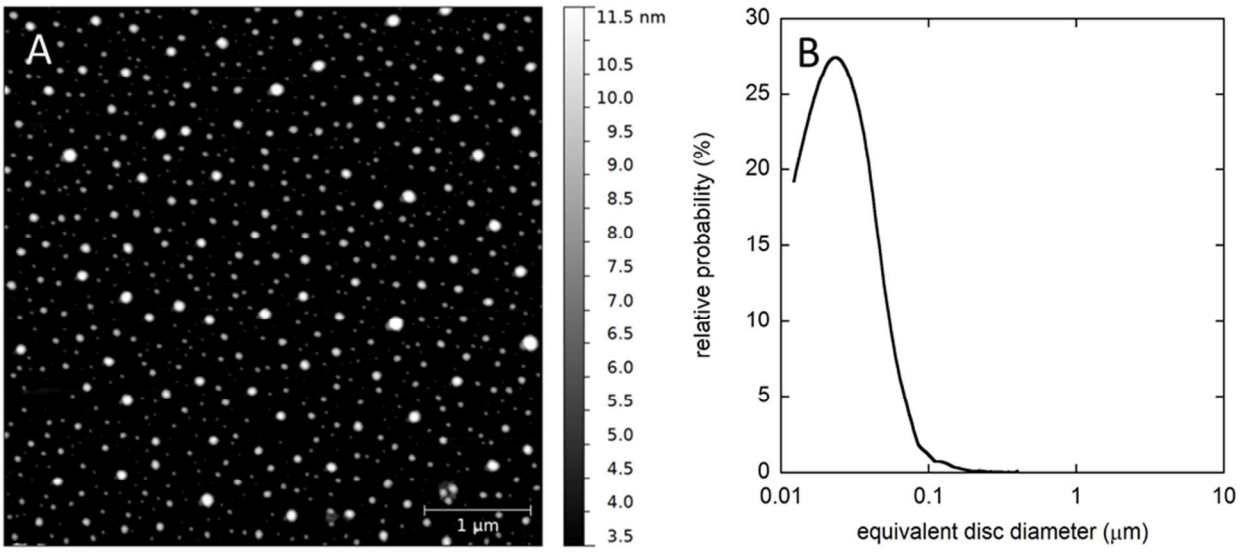

Figure 5. Panel A: AFM image of a naked NPs sample prepared from a 100-fold diluted solution. Panel B: size distribution profile obtained from the picture reported in Panel A.

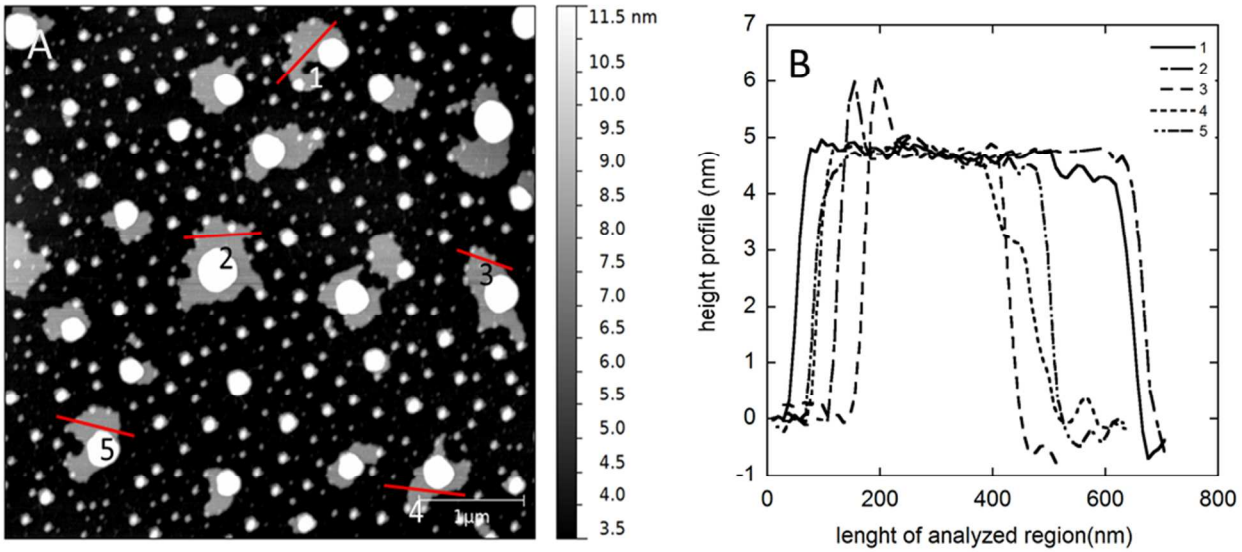

Figure 6. Panel A: AFM image of a membrane-coated NPs sample prepared from a 100-fold diluted solution from the stock. The numbered lines in the picture represent the regions whose profiles have been analyzed in Panel B. Panel B: height profiles of the regions indicated in Panel A.

Enzyme encapsulation

Quantification of the encapsulated enzyme

The quantification of the encapsulated enzyme fraction was obtained by exploiting the intrinsic SOD fluorescence[41] (see SI for details) based on the acquisition of a calibration curve with increasing SOD amounts. For this experiment, two stocks of NPs were prepared. In the first one a 4 mg/ml solution of SOD was included, while the second was synthesized without the enzyme; the spectra of the second solution were used for background subtraction in the fluorescence measurements. Before any purification, a spectrum was recorded from the stock solution (Figure 3, left panel). In this case, the value of SOD concentration is known from the conditions used in the synthesis (12.8 μM, SOD monomer), but it was anyway assessed with fluorescence, resulting in a comparable value (12.6 μM). Subsequently, a first dialysis was carried out maintaining the lipid bilayer integrity, to remove SOD from the extravesicular space (Figure 3, central panel). The spectrum obtained from this experiment indicated that the encapsulated enzyme fraction corresponded to 37% of the total SOD amount (Figure 7, Panel A). This result was confirmed by Cu and Zn atomic absorption experiments on an independent NPs sample, from which an average value of 34%±6% was obtained. The activity of this sample was practically not detectable, confirming that free SOD was efficiently removed from the NPs suspension (since the protein enclosed inside the phospholipid vesicle cannot exert its activity).[43]

After the addition of SDS to disrupt the bilayer (Figure 3, right panel), the sample was subjected to further dialysis cycles (lasting 24 hours each), showing a slow, partial release of the protein, without any undesirable initial burst phase (Figure 7, Panel A). This finding is in agreement with the FRAP experiments, which had shown that a fraction of the encapsulated protein was mobile and could be released over time. These data could be fitted with a first order kinetics with a lifetime of about 3 days and are compatible with the presence of a protein fraction that is not released even at very long times (around 30% of the encapsulated protein).

Enzymatic activity of the encapsulated enzyme

The activity of a NPs sample was measured directly after removal of the lipid bilayer by SDS addition, and was then followed for several days (Figure 7, Panel B). By contrast to the experiments reported in Panel A, in this case no further purification steps were performed, so that any enzyme released by the nanoparticles would remain in the sample. Control experiments on free SOD confirmed that the presence of the detergent does not affect the activity of the enzyme, as previously reported.[44]

The data in Figure 7 (Panel B) report the specific activity of the NPs sample (*i.e.* enzymatic units per mg of protein), normalized to that of a freshly prepared SOD solution (*i.e.* A/A_{free}, see SI). Immediately after membrane removal, the specific activity of the encapsulated protein was lower than that of the free, freshly prepared enzyme (about 35%). This finding could be due to different causes, including partial protein denaturation, inactivation by the radical polymerization reaction used to synthesize the gel, or a direct effect of the hydrogel matrix, *e.g.* on substrate diffusion or protein dynamics. However, a gradual increase in the sample activity was observed in the first days of the experiments (Figure 7, Panel B), with a rate comparable to that observed for enzyme release

from the NPs (Figure 7, Panel A). This observation indicates that the enzyme recovers its activity after release, and thus suggests that the reduced specific activity of the entrapped enzyme was due (at least in part) to reversible processes or to the NPs environment itself. Successively, the activity decreased, with a lifetime of 20 days, probably as a consequence of slow inactivation of the enzyme. However, a significant enzymatic activity was still present after 2 months.

The data of Figure 7 (Panel B) were analyzed with a model (see SI for details) assuming that a fraction of the encapsulated protein is stably entrapped inside the polymeric network, while another fraction (mobile) is able to diffuse out of the NPs, and that it recovers its full activity once free in solution, but then inactivates over time. From this analysis we determined the lifetime associated with the release processes and the fixed protein fraction (3 days and 37%, respectively), in good agreement with the data derived from protein quantification in an independent sample (Figure 7; Panel A).

After a total time of almost 6 months we tested again the enzymatic activity of the NPs and observed a value comparable to that of the 2 months-aged sample (data not shown), supporting the presence of a fixed fraction, which is highly resistant to denaturation.

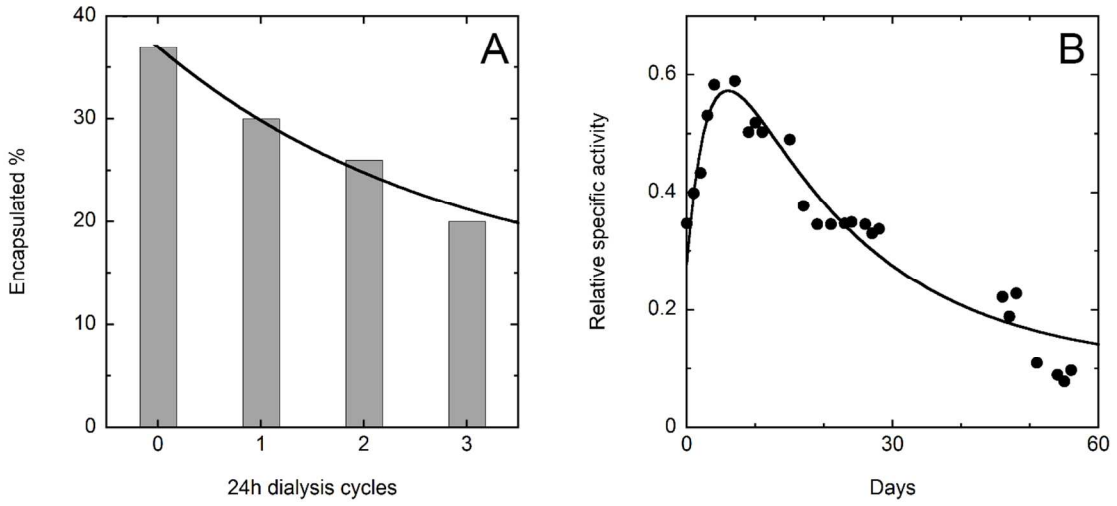

Figure 7. Panel A: Percentage of the total SOD used in the synthesis encapsulated inside the NPs, immediately after purification, and after successive cycles of dialysis, 24 h each. The continuous line represents an exponential fit to the data. Panel B: Variations in the specific activity of SOD in a naked, purified NPs sample normalized with respect to that of a freshly prepared SOD solution, as a function of time.

Enzyme stabilization

A further proof of the stabilizing effect of the NPs was provided by thermal degradation experiments, carried out on free SOD and on SOD-containing NPs. Samples were heated at 80°C and the enzyme activity was tested at different times. As reported in Figure 8, in the case of free SOD more than 50% of activity was lost in a few minutes. The activity decrease was much less evident for NPs-encapsulated SOD: in this case, the reduction was only about 6% of the initial activity, in the same time-range.

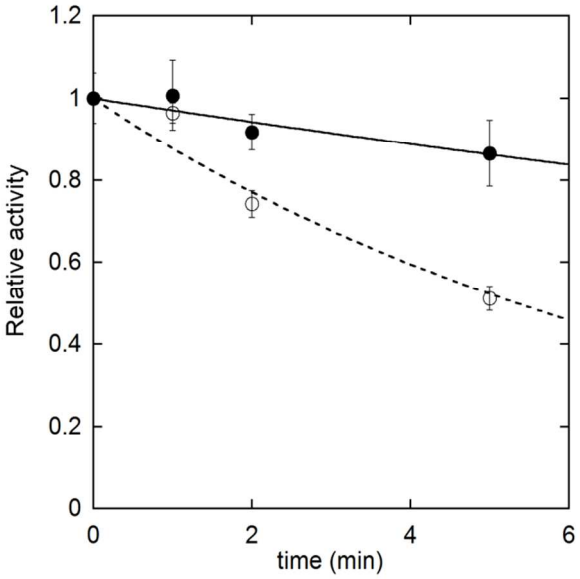

Figure 8. SOD thermal inactivation. Enzymatic activity of free SOD (empty circles, dotted line) and of NPs-encapsulated SOD (full circles, solid line). The heating temperature was 80 °C, and the activity was measured at T=25 °C after rapid cooling in an ice bath.

NPs-cell interaction

Cell viability assays

The biocompatibility of NPs is a fundamental requirement for their therapeutic application. Although the biocompatibility of polyacrylamide-based gels is well established[16,18,31] the potential toxicity of the samples used in this work was tested on cell cultures. The cell viability assays were performed using NPs which did not contain SOD, to detect exclusively the possible toxic effects of the vehicle.

The trypan blue assay is a test for cell membrane integrity and cell viability (see SI for details). According to this test, 99±1% and 93±6% of the cells were viable in the non treated control cultures and in cell cultures incubated for 24 hours with a 0.35 nM solution of NPs, respectively.

This finding indicates that NPs do not interfere significantly with cell integrity; this result was confirmed by the LIVE/DEAD assay, which assesses both membrane integrity and the enzymatic activity of the intracellular enzyme esterase (see SI for details). Also in this case, no relevant differences were observed between the control cell culture and the cell culture treated with NPs after incubation for 48 hours (Figure 9).

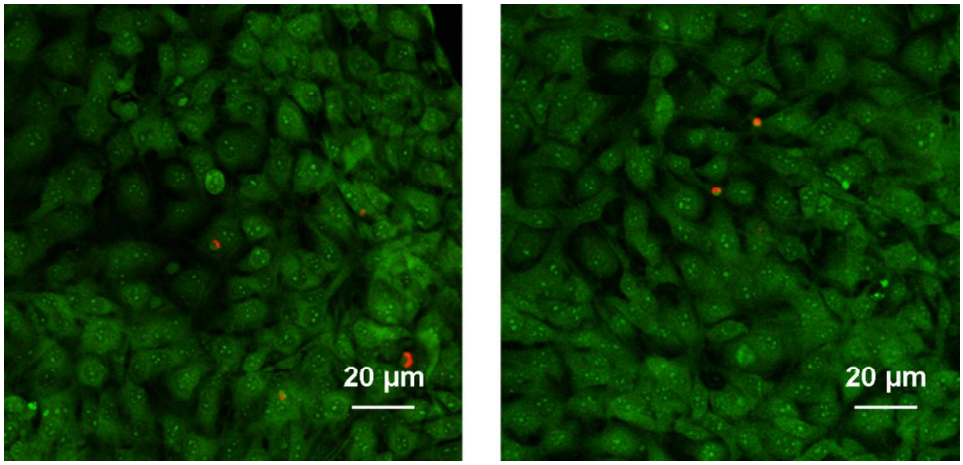

Figure 9. Confocal image of the control cell culture (left panel) and of the cell culture treated with naked NPs (not containing the SOD enzyme) (right panel) in the LIVE/DEAD assay after 48 hours of incubation.

Cell uptake experiments

In order to visualize NPs inside the cells to verify their uptake, fluorescein-labeled acrylamide (FLAC) has been synthesized as described in SI, and used to label NPs (not containing SOD) at a 5% molar ratio. We hypothesize that the absence of the enzyme or the presence of the fluorophore does not significantly influence the cell uptake of the NPs. Murine fibroblasts NIH3T3 were incubated with a 0.35 nM solution of fluorescent NPs. Both membrane-coated and naked NPs were efficiently internalized by cells already after 24 hours (Figure 10), as shown by the FLAC green fluorescence signal inside cells.

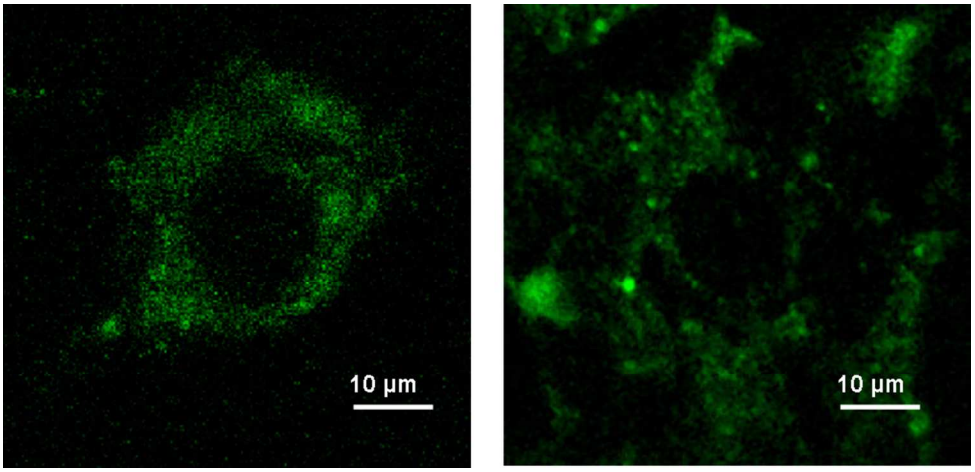

Figure 10. Confocal image of a fibroblast culture after a 24-hours incubation with a solution of membrane-coated (left panel) or naked (right panel) NPs (not containing SOD).

Generalizability of the proposed approach

To verify if the proposed method is generalizable, we synthesized NPs entrapping another enzyme, *i.e.* lactoperoxidase (LPO). This hemoprotein has a molecular weight of 77.5 kDa, and catalyzes the oxidation of a number of inorganic and organic substrates by hydrogen peroxide. Its enzymatic function plays a fundamental role in innate immunity, due to the strong antimicrobial activity of the short-lived oxidation products of LPO-catalyzed oxidation of thiocyanate. For this reason, LPO is investigated for the treatment of bacterial and viral infections[45]. In principle, a combination of SOD- and LPO-entrapping NPs could find application also in antioxidant therapies, with the two enzymes acting in cascade to degrade superoxide and H_2O_2[27]

As LPO is more susceptible than SOD to denaturation, we explored also the possibility to avoid or modify the steps of the NPs preparation protocol that are potentially damaging to enzymes. In the case of LPO, liposome extrusion was successfully performed without previous freeze-thaw

cycles (see SI), and the non-denaturing detergent CHAPS (3-[(3-cholamidopropyl)dimethylammonio]-1-propanesulfonate) was used in place of SDS.

The properties of the obtained NPs were similar to those of the SOD preparations described above. NPs had an average diameter of ~200 nm, enzyme encapsulation efficiency was 37% (as determined from the LPO intrinsic Trp fluorescence) and the specific activity of the encapsulated protein (immediately after membrane removal) was 41% of that of the free, freshly prepared enzyme.

DISCUSSION

The huge therapeutic potential of enzymes is still poorly exploited due to the many problems involved in their administration and delivery. In this work, a novel approach has been presented that can contribute to solve part of these issues.

Hydrogel NPs are considered promising vectors for protein-based drugs: they can increase the half-life of proteins in the body, avoiding the action of proteolytic enzymes, the interaction of antibodies with the entrapped enzyme, and rapid clearance from the organism.[46,2,47,16,48] However, all these advantages are partially lost when the protein is released, as required in most currently available hydrogel-based delivery vehicles, to allow the enzyme to exert its activity. By contrast, in our NPs the enzyme can exert its catalytic function even while it is still protected in its nanometric cage.

Our protocol produced a good encapsulation efficiency of about 37%, which depends on the relatively high lipid concentration used in the first step of the preparation (100 mM). The entrapment efficiency would be further increased for NPs of larger size, since the volume/surface ratio of a sphere increases with size, and therefore by forming larger vesicles the same amount of lipids can encapsulate a larger fraction of the solution volume. The size of the particles produced in this study (of the order of 100-200 nm) is in the optimal range to maximize circulation in the body

and enhanced permeation retention in tumor tissues.[49-51] However, the dimensions of the nanodevice must be tailored to each specific therapeutic application, and nanodevices of different sizes might be better suited in particular instances. One of the advantages of liposome-templated synthesis is the ease of variation of NPs radius during the extrusion step. Another important advantage of the NPs presented in this work is that synthesis in liposome nanotemplates allows the use of an acqueous environment during the entire process. In addition, the synthetic protocol proposed here produces NPs covered by a lipid bilayer, which can be used for further functionalization for active targeting, to improve the intracellular delivery of the nanodevice, or to avoid protein leakage during storage.

The mesh size of the hydrogel blocked effectively the SOD molecules, while maintaining a large fraction of their activity. Release of the proteins from the NPs matrix was very slow (with a lifetime of about 3 days), and a fraction of the protein was still encapsulated even at much longer times. These aspects could be probably improved even more by further optimization of the hdyrogel mesh size and components. In addition, it is worth mentioning that the release process starts only after membrane removal. Thus, the lipid membrane can be used to protect the NPs during the storage period, removing it only immediately before use (when needed).

In our preparation, the specific activity of the entrapped enzyme was only partially reduced (35% of that of the free enzyme). In principle, this finding could have several different causes. One possibility is protein modification by chemical reactions involving the highly active radical species generated during the photopolymerization process.[52] Control experiments showed that UV irradiation *per se* did not inactivate the protein. This finding is relevant also for potential therapeutic applications, since it shows that the NPs could be easily sterilized (even after synthesis) by UVC irradiation.[53] Most importantly, in our case the limited loss of enzymatic activity was reversed when the protein was freed from the hydrogel matrix, as previously observed in other similar instances[54].

This finding rules out any irreversible process, and indicates that the partially reduced specific activity of the NPs-entrapped protein was likely due to the hydrogel matrix itself, which could slow down the diffusion of the enzyme substrates and products, or partially hinder protein dynamics.[41] On the other hand, the encapsulated enzyme was significantly protected against denaturation, probably as a consequence of protein confinement in the hydrogel matrix, which reduces the entropy of the unfolded state through excluded volume effects.[55] This finding is in agreement with previous studies, which showed an enhancement of protein thermal stability in polyacrylamide gels with a pore size of 10 nm or less.[55]

Overall, the efficient protein entrapment, the slow release kinetics, the increased thermal stability of the entrapped enzyme and its potential protection from degradation bear well for the bioavailability and shelf life of this formulation. These properties are also promising for several potential industrial and technological applications,[56] where often enzymes have to face severely harsh conditions.

It is interesting to compare our system with vesicles formed by block copolymers, which have also been used to entrap enzymes such as SOD or LPO. [27]. In this devices, SOD was able to exert its activity without being released, because superoxide was able to diffuse through the polymeric shell. However, in the case of LPO penetration of the substrates in the aqueous lumen of the vesicles was obtained only by using porins, proteins that insert in the polymeric membrane and allow the passage of molecules with MW<600 Da. However, in this way the enzyme is protected, but other proteins (the porins themselves) are exposed on the surface of the nanodevice. By contrast, our experiments showed that the substrate used in our assay for LPO activity, which has a molecular weight of 500 Da, was able to diffuse through the meshes of the hydrogel, without the need for any further modification of the NPs. It can therefore be envisaged that the NPs presented here could be used also for the entrapment of several other therapeutically relevant enzymes.

Different assays demonstrated a good biocompatibility of our NPs, in agreement with previous studies on polyacrylamide-based hydrogels.[18,31] In the approach proposed in this study, biodegradability of the NPs is not desired, since the enzyme can exert its activity while still protected by the hydrogel. This is one of the reasons why polyacrylamide was selected for the synthesis of the NPs. It has been demonstrated that polyacrylamide hydrogels with the same composition of our NPs are strongly resistant to degradation: no acrylamide release was detected from gels stored at room temperature and exposed to artificial lights for 60 days.[57] Thus, the leakage of the toxic monomer inside the organism seems to be unlikely even for a long permanence in the body. In addition, several studies demonstrated that polyacrylamide NPs are eventually excreted by the organism through the feces, even though this process may require from several days to months.[58-60]

CONCLUSIONS

The nanodevice proposed in the present work is endowed with several desirable properties: it allows the enzyme to function even without being released; it is synthesized in an aqueous environment that maintains most of the enzyme activity; its size is easily tunable; it is covered by a phospholipid bilayer, which can be removed, or maintained to improve its stability during storage and its interaction with cellular membranes; it stabilizes the entrapped enzyme due to excluded volume effects; it allows a good encapsulation efficiency. All these characteristics make the NPs presented here a promising system, worth of further investigation as an alternative approach for delivery of enzyme-based therapies.

ASSOCIATED CONTENT

Supporting information available: materials and methods. This material is available free of charge via the internet at http://pubs.acs.org.

ACKNOWLEDGEMENTS

This research was supported by the Italian Ministry of Education, University and Research (PRIN project). The authors are grateful to Prof. Giovanni Antonini and Dr. Loris Leboffe for making the LPO enzyme available, to Prof. Massimo Bietti and Dr. Michela Salamone for help with the FLAC synthesis and for the use of the photoreactor, to Dr. Elena Romano for assistance in FRAP experiments, to Dr. Lorenzo Tancioni for the use of the osmometer and to Prof. Gianfranco Bocchinfuso and Prof. Andrea Battistoni for helpful discussions.

REFERENCES

1 Vellard, M. The enzyme as drug: application of enzymes as pharmaceuticals. *Curr. Opin. Biotechnol.* **2003**, *14*, 444-450.

2 Grabowski, G.A.; Hopkin, R.J. Enzyme therapy for lysosomal storage disease: principle, practice, and prospects. *Annu. Rev. Genomics Hum. Genet.* **2003**, *4*, 403-436.

3 Torchilin, V. Peptide and protein drug delivery to and into tumors: challenges and solutions. *Drug Discovery Today* **2003**, *8*, 259-266.

4 Nalivaeva, N. N.; Beckett, C.; Belyaev, N. D.; Turner, A. J. Are amyloid-degrading enzymes viable therapeutic targets in Alzheimer's disease? *J. Neurochem.* **2012**, *120*, 167-185.

5 O'Brady, R.; Schiffmann, R. *Enzyme-replacement therapy for metabolic storage disorders. The Lancet Neurology* **2004**, *3*, 752-756.

6 van de Weert, M. and Moeller, E. H. Eds, in *Immunogenicity of biopharmaceuticals*. Springer Publications, New York, Usa, 2008.

7 Frokjaer, S.; Otzen, D. E. Protein drug stability: A formulatioin challenge. *Nat. Rev. Drug Discovery* **2005**, *4*, 298-306.

8 Bysell, H.; Månsson, R.; Hansson, P.; Malmsten, M. Microgels and microcapsules in peptide and protein drug delivery. *Adv. Drug. Delivery. Rev.* **2011**, *63*, 1172-1185.

.

9 M. Ye, S. Kim and K. Park, Issues in long-term protein delivery using biodegradable microparticles. *J. Controlled Release* **2010**, *146*, 241-260.

10 Kazakov, S.; Kaholek, M.; Teraoka, I.; Levon, K. UV-induced gelation on nanometer scale using liposome reactor. *Macromolecules* **2002**, *35*, 1911-1920.

11 An, S. Y.; Bui, M. P. N.; Nam, I. J.; Kwi, N. H.; Li, L. A.; Choo, J.; Lee, E.Y.; Katoh, S.; Kumada, Y.; Seong, G. H. Preparation of monodisperse and size-controlled poly(ethileneglycol) hydrogel nanoparticles using liposome templates. *J. Colloid Interface Sci.* **2009**, *331*, 98-103.

12 Patton, J. N.; Palmer, A. F. Photopolymerization of Bovine Hemoglobin Entrapped Nanoscale Hydrogel Particles within Liposomal Reactors for Use as an Artificial Blood Substitute. *Biomacromolecules* **2005**, *6*, 414-424.

13 Patton, J. N.; Palmer, A. F. Engineering Temperature-Sensitive Hydrogel Nanoparticles Entrapping Hemoglobin as a Novel Type of Oxygen Carrier. *Biomacromolecules* **2005**, *6*, 2204-2212.

14 Kazakov, S.; Kaholek, M.; Levon, K. Nanogels and their production using liposomes as reactors. Patent WO 2003015936 A1

15 van Thienen, T. G.; Raemdonck, K.; Demeester, J.; De Smedt, S. C. Protein Release from Biodegradable Dextran Nanogels. *Langmuir* **2007**, *23*, 9794-9801.

16 Delgado, M.; Spanka, C.; Kervin, L.D.; Wentworth, P. J.; Janda, K. A Tunable Hydrogel for Encapsulation and Controlled Release of Bioactive Proteins. *Biomacromolecules* **2002**, *3*, 262-272.

17 Sairam, M.; Babu, V. R.; Naidu, B. V. K.; Aminabhavi T. M. Encapsulation efficiency and controlled release characteristics of crosslinked polyacrylamide particles *Int. J. Pharm.* **2006**, *320,* 131-136.

18 Kadajji, V.G.; Betageri, G.V. Water Soluble Polymers for Pharmaceutical Applications *Polymers* **2011**, *3*, 1972-2009.

19 McCord, J.; Fridovich, I. Superoxide dismutase. An enzymic function for erythrocuprein (hemocuprein). *J. Biol. Chem.* **1969**, *244*, 6049-6055.

20 Muscoli, C.; Cuzzocrea, S.; Riley, D. P.; Zweier, J. L.; Thiemermann, C.; Wang, Z.Q.; Salvemini, D. On the selectivity of superoxide dismutase mimetics and its importance in pharmacological studies. *Br. J. Pharmacol.* **2003**, *140*, 445-460.

21 Perry, J. J. P.; Shin, D. S.; Getzoff, E. D.; Tainer, J. A. The structural biochemistry of superoxide dismutase. *Biochim. Biophys. Acta* **2010**, *1804*, 245-262.

22 Veronese, F. M.; Caliceti, P.; Schiavon, O.; Sergi, M. Polyethylene glycol–superoxide dismutase, a conjugate in search of exploitation. *Adv. Drug Delivery Rev.* **2002**, *52*, 587–606.

23 Cruz, M. E. M.; Gaspar, M. M.; Martins, M. B. F.; Corvo, M.L. Liposomal superoxide dismutases and their use in the treatment of experimental arthritis. *Methods Enzymol.* **2005**, *413*, 391-395.

24 Giovagnoli, S.; Luca, G.; Casaburi, I.; Blasi, P.; Macchiarulo, G.; Ricci, M.; Calvitti, M.; Basta, G.; Calafiore, R.; Rossi, C. Long-term delivery of superoxide dismutase and catalase entrapped in poly(lactide-co-glycolide) microspheres: In vitro effects on isolated neonatal porcine pancreatic cell clusters. *J. Controlled Release* **2005**, *107*, 65-77.

25 Çelik, Ö.; Akbuğa, J. Preparation of superoxide dismutase loaded chitosan microspheres: Characterization and release studies *Eur. J. Pharm. Biopharm*. **2007**, *66*, 42–47.

26 Corvo, M. L.; Boerman, O. C.; Oyenm, W. J. G.; Van Bloois, L.; Cruz, M. E. M.; Crommelin, D. J. A.; Storm, G. Intravenous administration of superoxide dismutase entrapped in long circulating liposomes: II. In vivo fate in a rat model of adjuvant arthritis. *Biochim. Biophys. Acta, Biomembr*. **1999**, *1419*, 325-334.

27 Tanner, P.; Balasubramanian, V.; Palivan, C.G. Aiding nature's organelles: artificial peroxisomes play their role. *Nano Lett.* **2013**, *13*, 2875−2883.

28 Baumann, G.; Chrambach, A. A highly crosslinked, transparent polyacrylamide gel with improved thermal stability for use in isoelectric focusing and isotachophoresis. *Anal. Biochem.* **1976**, *70*, 32-38.

29 Baselga, J.; Hernansez-Fuentes, I.; Pierola, I. F.; Llorente, M. A. Elastic properties of highly-crosslinked polyacrylamide gels. *Macromolecules* **1987**, *20*, 3060-3065.

30 Nagash, H. J.; Okay, O. *Formation and structure of polyacrylamide gels. J. Appl. Polym. Sci.* **1996**, *69*, 971-979.

31 Saraydin, D.; Ünver-Saraydin, S., Karadag, E.; Koptagel, E.; Güven, O. In vivo biocompatibility of radiation crosslinked acrylamide copolymers. *Nucl. Instrum. Methods Phys. Res. Sect. B* **2004**, *217*, 281-292.

32 Rodriguez-Diaz, R.; Wehr, T.; Tuck, S. Eds, In *Analytical techniques for biopharmaceutical development*. CRC Press, USA 2005.33 Rodbard, D.; Levitov, C.; Chrambach, A. Electrophoresis in Highly Cross-linked Polyacrylamide Gels. *Sep. Sci.* **1972**, *7*, 705-723.

34 Stellwagen, N. C. Apparent pore size of polyacrylamide gels: comparison of gel cast and run in Tris-acetate EDTA and Tris-borate EDTA buffers. *Electrophoresis* **1998**, *19*, 1542-1547.

35 Shi, Q.; Jackowski, G. In *Gel electrophoresis of proteins, a practical approach. B.*, D. Hames, D. Rickwood Eds., Oxford University Press, UK 1998.

36 Asnaghi, D.; Giglio, M.; Bossi, A; Righetti, P. G. Quasi-ordered structures in highly cross-linked poly(acrylamide) gels. *Macromolecules* **1997**, *30*, 6194-6198.

37 Lira, L. M.; Martins, K. A.; Cordoba de Torresi, S. I. Structural parameters of polyacrylamide hydrogels obtained by the equilibrium swelling theory. *Eur. Polymer J,* **2009**, *45*, 1232–1238.

38 Russell, S. M.; Carta, G. Mesh size of charged polyacrylamide hydrogels from partitioning measurements. *Ind. Eng. Chem. Res.* **2005**, *44*, 8213-8217.

39 Damodaran, S.; Song, K. B. Diffusion and Energy Barrier Controlled Adsorption of Proteins at the Air-Water Interface. *Inter. Food Prot.* **1991**, 8, 104–121.

40 Salin, M. L.; Wilson, W. W. Porcine superoxide dismutase. *Mol. Cell. Biochem.* **1981**, *36*, 157-161.

41 Ferreira, S.T.; Stella, L.; Gratton, E. Conformational dynamics of bovine Cu, Zn superoxide dismutase revealed by time-resolved fluorescence spectroscopy of the single tyrosine residue. *Biophys J.* **1994**, *66*, 1185-96.

42 Berger, N.; Sachse, A.; Bender, J.; Schubert, R.; Brandl, M. Filter extrusion of liposomes using different devices: comparison of liposome size, encapsulation efficiency, and process characteristics. *Int. J. Pharm.* **2001**, *223*, 55-68.

43 Dong Mao, G.; Poznansky M.J. Electron spin resonance study on the permeability of superoxide radicals in lipid bilayers and biological membranes. FEBS LETT. **1992**, *305,* 233-236.

44 Manning, M.; Colon, W. Structural Basis of Protein Kinetic Stability: Resistance to Sodium Dodecyl Sulfate Suggests a Central Role for Rigidity and a Bias Toward β-Sheet. Structure *Biochemistry.* **2004**, *43*, 11248–11254

45 Thallinger, B.; Prasetyo, E.N.; Nyanhongo, G.S.; Guebitz, G.M. Antimicrobial enzymes: an emerging strategy to fight microbes and microbial biofilms. *Biotechnol. J.* **2013**, *8*, 97–109.

46 Martins, S.; Sarmento, B.; Ferreira, D.C.; Souto, E. B. Lipid-based colloidal carriers for peptide and protein delivery-liposomes versus lipid nanoparticles. *Int. J. Nanomed.* **2007**, *2*, 596-607.

47 De Groot, A. S.; Scott, D. W., Immunogenicity of protein therapeutics. *Trends Immunol.*, **2007**, *28*, 482-490.

48 Peppas, N. A.; Hilt, J. Z.; Khademhosseini, A.; Langer, R. Hydrogels in Biology and Medicine: From Molecular Principles to Bionanotechnology. *Adv. Mater.* **2006**, 18, 1345-1360.

49 Alexis, F.; Pridgen, E.; Molnar, L.K.; Farokhzad, O.C. Factors affecting the clearance and biodistribution of polymeric nanoparticles. *Mol. Pharmaceutics,* **2008**, *5*, 505-515.

50 Liu, D.; Mori, A.; Huang, L. Role of liposome size and RES blockade in controlling biodistribution and tumor uptake of GM1-comtaining liposomes. *Biochim. Biophys. Acta, Biomembr.,* **1992**, *1104*, 95-101.

51 Raemdonck, K.; Braeckmans, K.; Demeester, J., De Smedt, S. C. Merging the best of both worlds: hybrid lipid-enveloped matrix nanocomposites in drug delivery. *Chem. Soc. Rev.*, **2014**, *43*, 444-472.

52 Lin, C. C.; Sawicki, S. M.; Metters, A. T. Enhanced protein delivery from photopolymerized hydrogels using a pseudospecific metal chelating ligand. *Biomacromolecules,* **2008**, *9*, 75–83.

53 Cerroni, B. ; Chiessi, E. ; Margheritelli, S. ; , L. Oddo, L. ; Paradossi, G. Polymer Shelled Microparticles for a Targeted Doxorubicin Delivery in Cancer Therapy. *Biomacromolecules*, **2011**, *12*, 593-601

54 Censi, R. ; Vermonden, T. ; van Steenbergen, M. J. ; Deschout, H. ; Braeckmans, K. ; De Smedt, S. C. ; van Nostrum, C. F.; di Martino, P. ; Hennink, W. E. Photopolymerized thermosensitive hydrogels for tailorable diffusion-controlled protein delivery *J. Controlled Release* **2009**, *140*, 230-236

55 Bolis, D.; Politou, A. S.; Kelly, G.; A. Pastore, A.; Temussi, P. A. Protein stability in nanocages: a novel approach for influencing protein stability by molecular confinement. *J.Mol. Biol.* **2004**, *336*, 203-212.

56 van Beilen, J. B.; Li, Z. Enzyme technology: an overview. *Curr. Opin. Biotechnol.* **2002**, *13*, 338–344.

57 Calfield, M. J.; Hao, X.; Qiao, G. G.; Solomon, D. H. Enzyme technology: an overview. *Polymer* **2003**, ***44***, 3817-3826.

58 Liu, Y. ; Ibricevic-Richardson, A. ; Cohen, J. A. ; Cohen, J. L. ; Gunsten, S. P. ; Fréchet, J. M. J. ; Walter, M. J. ; Welch M. J. ; Brody, S. L. Impact of Hydrogel Nanoparticle Size and Functionalization on In Vivo Behavior for Lung Imaging and Therapeutics. *Mol. Pharm.* **2009**, *6*, 1891.

59 Kreuter, J. Nanoparticle-based dmg delivery systems. *J. Controlled Release,* **1991**, *16*, 169-176.

60 Wenger, Y. ; Schneider, R. J. Reddy, R. ; Kopelman, R. ; Jolliet, O.; Philbert, M. A. Tissue distribution and pharmacokinetics of stable polyacrylamide nanoparticles following intravenous injection in the rat. *Toxicol. Appl. Pharmacol.* **2011**, *251*, 181-190.

TABLE OF CONTENTS GRAPHICS